

Average Minimum Distances of periodic point sets

Daniel Widdowson

Department of Computer Science, University of Liverpool, Liverpool, United Kingdom
D.E.Widdowson@liverpool.ac.uk

Marco Mosca

Department of Computer Science, University of Liverpool, Liverpool, United Kingdom
m.m.mosca@liverpool.ac.uk

Angeles Pulido 

Cambridge Crystallographic Data Centre, Cambridge, United Kingdom
apulido@ccdc.cam.ac.uk

Vitaliy Kurlin 

Department of Computer Science, University of Liverpool, Liverpool, United Kingdom
vitaliy.kurlin@liverpool.ac.uk

Andrew I Cooper

Materials Innovation Factory, University of Liverpool, Liverpool, United Kingdom
aicooper@liverpool.ac.uk

Abstract

Periodic sets of points model all solid crystalline materials (crystals) by representing atoms as labeled points. Crystal structures are determined in a rigid form and are considered up to rigid motions or isometries. Modern tools of Crystal Structure Prediction output thousands of simulated structures, though only few of them can be really synthesized. The first obstacle is the presence of many near duplicate structures that can not be efficiently recognized on the fly by past tools. To continuously quantify a similarity between periodic sets, their isometry invariants should be continuous under perturbations when all discrete invariants such as symmetry groups can break down. This paper studies the isometry classification problem for periodic sets with the new continuity requirement and introduces the Average Minimum Distances, which form an infinite sequence of continuous isometry invariants. Their asymptotic behaviour for a wide class of sets is explicitly described in terms of a point packing coefficient. All results are illustrated by experiments on large datasets of crystals.

2012 ACM Subject Classification Theory of computation → Computational geometry

Keywords and phrases Lattices, periodic point sets, isometries, bottleneck distance, stability

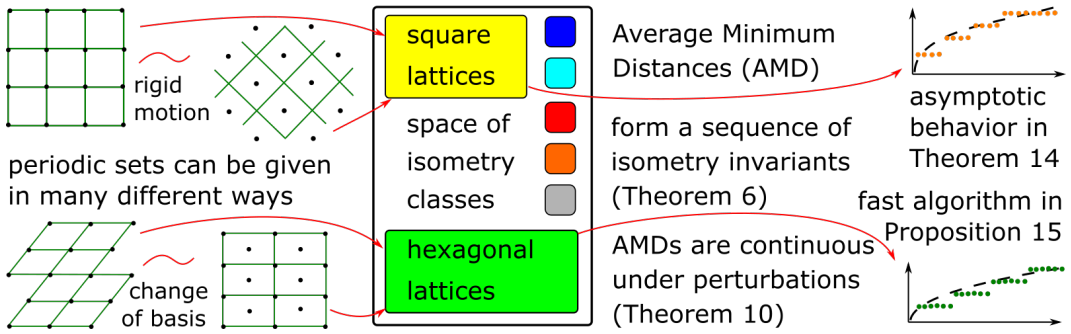
Funding *Vitaliy Kurlin*: EPSRC grant ‘Application-driven Topological Data Analysis’, EP/R018472/1
Andrew I Cooper: ERC Synergy Grant ‘Autonomous Discovery of Advanced Materials’

1 Motivations, problem statements and overview of main results

A periodic crystal is obtained by periodically translating a finite motif of atoms along vectors of a lattice generated by a linear basis [20]. Any atom can be modeled as a point labeled by a chemical element or a radius or another property. Any real crystal is represented by a periodic set of labeled points. The addition sign below refers to a Minkowski sum of sets.

A *periodic point set* = (a lattice given by a basis) + (a motif of labeled points), see Fig. 1.

Representing a periodic set as a sum of a lattice and a motif is highly ambiguous, because one can choose infinitely many bases with different motifs that define the same crystal. Since crystal structures are determined in a rigid form, they should be considered up to rigid motions or *isometries* that preserve interpoint distances [11]. A *crystal* should be defined as an *isometry class* = {periodic point sets equivalent up to (a change of a basis) \times (isometry)}.



■ **Figure 1 Left** : all unit square lattices are isometric to each other, the hexagonal lattice in the bottom can be given by a rectangular basis with a motif of two points (one corner and one centre). **Middle** : isometry classes of periodic sets form a continuous space. **Right** : isometry classes can be distinguished only by invariants. Average Minimum Distances are introduced in Definition 5.

The multiplication sign above refers to compositions of isometries and changes of a basis, which act on a periodic point set and a motif of points in a fixed lattice, respectively [20]. We consider all isometries including reflections that reverse an orientation, because specifying an orientation is easier than distinguishing periodic point sets up to all general isometries.

If we add edges between points in a periodic set, we get a periodic graph. In practice, these edges can be justified only for strong covalent bonds in molecular crystals. Most chemical bonds are weak and are often displayed by using disputed thresholds on distances and angles. So bonds are abstract interactions between clouds of electrons, while atomic positions are better defined. The green lines in Fig. 1 only help to visualize lattices, which consists of points. We will study the fundamental case of periodic point sets without edges.

► **Problem 1** (isometry classification). Find an isometry invariant I of periodic sets that is (1) continuous under perturbations in the bottleneck distance, (2) computable in a near linear time in the size of a motif, (3) complete: if $I(S) = I(Q)$, then S, Q are isometric.

The *bottleneck distance* $d_B(S, Q)$ between periodic sets $S, Q \subset \mathbb{R}^n$ is $\sup_{a \in S} |a - g(a)|$ minimized over bijections $g : S \rightarrow Q$. The continuity of an isometry invariant I means that a suitable distance between $I(S), I(Q)$ is bounded above by $Cd_B(S, Q)$ for a constant C .

This paper contributes the following results to the *isometry classification*, motivated by the practical need to continuously quantify similarities between crystals, see appendix B.

- Proposition 4 gives an algorithmic criterion to detect homometric sets that are hard to distinguish by traditional crystallographic tools including powder X-ray diffraction patterns.
- Definition 5 introduces the Average Minimum Distance $AMD_k(S)$ of a periodic point set S . If S is a lattice, $AMD_k(S)$ is the distance from the origin to the k -th nearest point in S . If S is a periodic set, $AMD_k(S)$ is the average of k -th shortest distances over all motif points.
- Theorem 6 shows that $AMD_k(S)$ is invariant under isometries and changes of a basis.
- Theorem 10 proves that $AMD_k(S)$ continuously change under any bounded perturbations.
- By Theorem 14 the invariants $AMD_k(S)$ become asymptotically proportional to $\sqrt[k]{k}$ as $k \rightarrow \infty$ with a coefficient depending on a density of a periodic point set $S \subset \mathbb{R}^n$.
- Proposition 15 provides a fast algorithm to compute Average Minimum Distances up to an index k , whose complexity is near linear in k and the motif size m for a fixed dimension n .

2 Computational geometry background for periodic point sets

In Euclidean space \mathbb{R}^n , any point $p \in \mathbb{R}^n$ can be represented by the vector \vec{p} from the origin of \mathbb{R}^n to the point p , though \vec{p} can be drawn at any initial point. The *Euclidean* distance between points $p, q \in \mathbb{R}^n$ is denoted by $|pq| = |\vec{p} - \vec{q}|$. For a standard orthonormal basis $\vec{e}_1, \dots, \vec{e}_n$, the integer lattice $\mathbb{Z}^n \subset \mathbb{R}^n$ consists of all points with integer coordinates.

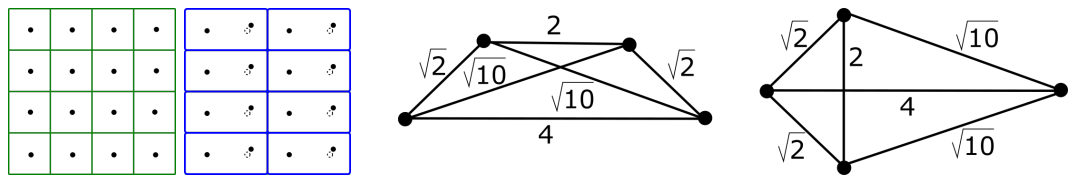
Definition 2 below models all atoms in crystals as zero-sized points, which is the most important basis case for isometry classification. To model real atoms, one can add labels for elements such as C for carbon, O for oxygen, etc. Geometrically, atoms can be modeled as weighted points, i.e. balls of different radii. We often call a *periodic point set* in \mathbb{R}^n simply a *periodic set*, while *crystals* refer only to dimension 3.

Any periodic point set S can be defined as a finite union of translates of a lattice Λ .

► **Definition 2** (a lattice Λ , a motif M , a unit cell U , a periodic set $S = \Lambda + M$). A *lattice* Λ in \mathbb{R}^n consists of all linear combinations $\sum_{i=1}^n \lambda_i \vec{v}_i$ with integer coefficients $\lambda_i \in \mathbb{Z}$. Here the vectors $\vec{v}_1, \dots, \vec{v}_n$ should form a *basis* so that if $\sum_{i=1}^n \lambda_i \vec{v}_i = \vec{0}$ for some real λ_i , then all $\lambda_i = 0$. A *motif* M is a finite set of points p_1, \dots, p_m in the *unit cell* $U(\vec{v}_1, \dots, \vec{v}_n) = \left\{ \sum_{i=1}^n \lambda_i \vec{v}_i : \lambda_i \in [0, 1] \right\}$, which is the parallelepiped spanned by $\vec{v}_1, \dots, \vec{v}_n$. A *periodic set* $S \subset \mathbb{R}^n$ is the *Minkowski* sum of a lattice Λ and a motif M , i.e. $S = \Lambda + M = \{u + v : u \in \Lambda, v \in M\}$. A unit cell U is *primitive* if S remains invariant under shifts by vectors only from Λ generated by U . ■

Any lattice Λ can be considered as a periodic set with a 1-point motif $M = \{p\}$. This single point p can be arbitrarily chosen in a unit cell U . The lattice translate $\Lambda + \vec{p}$ is also considered as a lattice, because the point p can be chosen as the origin of \mathbb{R}^n . The sets in the top left part of Fig. 1 represent the same isometry class of square lattices, though the former has a point p at a corner of a unit cell U and the latter has p in the center of U . The sets in the bottom left part of Fig. 1 represent the same isometry class of hexagonal lattices, because every black point has exactly six nearest neighbors that form a regular hexagon.

A lattice Λ of a periodic set $S = M + \Lambda \subset \mathbb{R}^n$ is not unique in the sense that S can be generated by a sublattice of Λ and a motif larger than M . For example, if U is any unit cell of Λ , the sublattice 2Λ has the 2^n times larger unit cell $2^n U$ (twice larger along each of n basis vectors of U), hence contains 2^n times more points than M . Such an extended unit cell $2^n U$ is superfluous, because S remains invariant under translations along not only $\sum_{i=1}^n \lambda_i \vec{v}_i$ with $\lambda_i \in \mathbb{Z}$, but also along linear combinations with half-integer coefficients $\lambda_i \in \frac{1}{2}\mathbb{Z}$.



► **Figure 2 Left:** the square lattice and its perturbation with a rectangular primitive cell are very close geometrically, so the volume of a primitive cell is discontinuous. **Right:** these non-isometric sets of four points can not be distinguished by all pairwise distances $\{2, \sqrt{2}, \sqrt{2}, \sqrt{10}, \sqrt{10}, 4\}$.

3 Closely related past work on comparisons of point sets and crystals

Now we discuss the closely related work about comparing finite and periodic sets up to isometries. The excellent book [14] reviews the wider area of distance geometry.

The full distribution of all pairwise Euclidean distances $|a - b|$ between points a, b in a finite set $S \subset \mathbb{R}^m$ is a well-known isometry invariant. This invariant is complete or injective for finite sets in a general position [6] in the sense almost any finite set can be uniquely reconstructed up to isometry from the set of all pairwise distances. However, the two pictures on the right hand side of Fig. 2 show a classical counter-example to the full completeness: two non-isometric 4-point sets have the same set of all six pairwise distances.

The isometry classification of finite point sets was algorithmically resolved by [2, Theorem 1] saying that an existence of an isometry between two m -point sets in \mathbb{R}^n can be checked in time $O(m^{n-2} \log m)$. The latest advance is the sophisticated $O(m \log m)$ algorithm [13] testing an isometry (or congruence) between m -point sets in \mathbb{R}^4 . However, these algorithms for finite point sets cannot be easily extended to periodic sets as discussed below.

A periodic crystal is stored as a Crystallographic Information File (CIF) including parameters of a unit cell (three edge-lengths and three angles in \mathbb{R}^3) and all atoms with chemical labels and fractional coordinates, which are coefficients of atomic centers in the vector basis of the unit cell. Many crystal descriptors depend on a unit cell or cut-offs or tolerances [12], hence are not isometry invariants. Though the average color of clothes can sometimes distinguish all people in a room, non-invariants cannot reliably identify humans.

A traditional method to check if two crystals are identical compares their finite motifs of atoms in reduced cells. The best example is Niggli's reduced cell [11, section 9.3], which is unique, but was shown to be discontinuous [3] in the sense that a reduced cell of a perturbed lattice can have a basis that substantially differs from that of a non-perturbed lattice.

The discontinuity under atomic vibrations is the major weakness of all discrete invariants including symmetry groups. The two nearly identical periodic sets on the left hand side of Fig. 2 should be recognizable as very similar. However, they have different symmetry groups and can be related only by approximate symmetries, which depend on various thresholds.

More than 40 years since the discovered discontinuity of reduced cells, the difficulty of comparing periodic sets is highlighted by the first author of [3] on their webpage [1]: "...find a measure of the difference between pairs of lattices. Surprisingly, this is not a mathematical problem with a well-defined solution". Our recent work [16] has resolved this problem for lattices by introducing two metrics that satisfy continuity under perturbations. This paper makes the next step by introducing continuous isometry invariants for periodic sets.

Though there is no justified distance that satisfies all metric axioms for any periodic crystals, the COMPACK algorithm [8] in the Mercury software is widely used for a pairwise comparison of crystals. Within given tolerances (20° for angles and 20% for distances), up to a given number (15 by default) of molecules from two crystals are matched by a rigid motion that

minimizes the Root Mean Square deviation of N matched atoms $\text{RMS} = \sqrt{\frac{1}{N} \sum_{i=1}^N |p_i - q_i|^2}$.

If a match between finite portions of periodic crystals is extended, RMS can also increase, potentially to infinity, e.g. between the cubic lattices of sizes 1 and 1.1. Table 1 shows how RMS depends on the maximum number m of attempted molecules to match by isometry.

m matched molecules	5 of 5	8 of 10	10 of 15	11 of 20	16 of 25	18 of 30	21 of 35
RMS, $1\text{\AA} = 10^{-10}m$	0.603	0.681	0.812	0.825	0.99	1.027	1.079

■ **Table 1** The Root Mean Square (RMS) deviation between the experimental T2- δ crystal [18] and its closest simulated version with ID 14. The irregular dependence of RMS on m makes this comparison unreliable. The computation for 35 molecules was about 1000 times longer than for 15.

The idea of the Average Minimum Distances (AMDs) in Definition 5 is close to the Radial Distribution Function (RDF), which measures the probability to find a number of atoms at a distance of r from a reference atom [11, vol. B, sec. 4.6]. The RDF is defined via a multidimensional integral, which is often approximated and visualized as a smooth function. Section 4 discusses *homometric* crystals, which have identical RDFs, but different AMDs.

4 A fast algorithm to detect homometric periodic sets of points

This section discusses homometric periodic sets that were hard to distinguish up to isometry, because they have identical diffraction patterns depending only on the difference set below.

► **Definition 3** (homometric sets). For any finite set $S \subset \mathbb{R}^n$ of m points, the *difference* multi-set $\text{Dif}(S)$ consists of the m^2 vector differences $\vec{a} - \vec{b}$ for all points $a, b \in S$, counted with multiplicities. Periodic point sets $S, Q \subset \mathbb{R}^n$ with a common lattice Λ and a primitive unit cell U are called *homometric* if $\text{Dif}(S \cap U) \equiv \text{Dif}(Q \cap U) \pmod{\Lambda}$ with multiplicities respected, i.e. all pairs of vectors $u \in \text{Dif}(S \cap U)$ and $v \in \text{Dif}(Q \cap U)$ that are equal up to lattice translations have the same multiplicity. ■

If a set S consists of m points, $\text{Dif}(S)$ includes the zero vector with multiplicity m . The above definition is updated in comparison with past attempts to define homometric sets.

Patterson [17, p.197] called periodic point sets $S, Q \subset \mathbb{R}^n$ *homometric* if $\text{Dif}(S \cap U) \equiv \text{Dif}(Q \cap U) \pmod{\Lambda}$ without mentioning weights or multiplicities. Franklin [10, equations (17)-(18)] renamed them as *homometric modulo a lattice* and called S, Q *homometric* if $\text{Dif}(S \cap U) = \text{Dif}(Q \cap U)$, not modulo Λ . Both definitions required that S, Q are not isometric. However, after removing this restriction, we expect to get an equivalence relation so that any periodic point set should be homometric to itself even if another unit cell is chosen. Example below shows that the equation $\text{Dif}(S \cap U) = \text{Dif}(Q \cap U)$ without lattice translations fails this reflexivity condition.

Franklin [10, p. 699] considered the sets $S_3 = \{0, 1\} + 3\mathbb{Z}$ and $Q_3 = \{0, 2\} + 3\mathbb{Z}$, which are isometric by $x \mapsto x + 1 \pmod{3}$. However, $\text{Dif}(\{0, 1\}) = \{0, 0, -1, +1\} \neq \text{Dif}(\{0, 2\}) = \{0, 0, -2, +2\}$. These sets are equal modulo 3, hence lattice translations are needed. If we consider S_3 with a twice larger unit cell and period 6, i.e. $S_3 = \{0, 1, 3, 4\} + 6\mathbb{Z}$, then

$$\text{Dif}(\{0, 1, 3, 4\}) = \{0, 0, 0, 0, \pm 1, \pm 1, \pm 2, \pm 3, \pm 4\}.$$

The above set can be considered equal to $\text{Dif}(\{0, 1\})$ modulo 3 only if the multiplicities in both sets are normalized so that their sums are equal. Hence Definition 3 requires a primitive unit cell U . Most importantly, Proposition 4 below justifies that homometry in Definition 3 is independent of a primitive unit cell and is an *equivalence* relation.

Proposition 4 makes the concept of homometric crystals algorithmic verifiable. It might be a folklore result, but we couldn't find the claim and a proof in the literature.

► **Proposition 4** (algorithm for homometric sets). (a) For any periodic point set $S \subset \mathbb{R}^n$ with a lattice Λ , the difference set $\text{Dif}(S \cap U) \pmod{\Lambda}$ does not depend on a primitive unit cell U of S . So the homometry in Definition 3 is an equivalence relation.

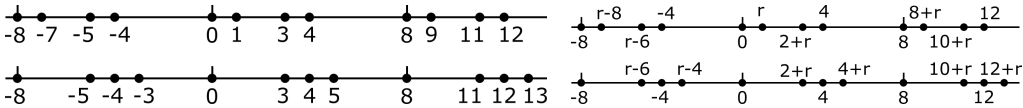
(b) Given a common primitive unit cell U containing m points of periodic point sets $S, Q \subset \mathbb{R}^n$, there is an algorithm of complexity $O(m^2 \log m)$ to determine if S, Q are homometric. ■

Proof. Let U, U' be primitive cells of the periodic set $S \subset \mathbb{R}^n$. Any point $q \in S \cap U'$ can be translated along a vector $\vec{v} \in \Lambda$ to a point $p \in S \cap U$ and vice versa. These translations establish a bijection $S \cap U \leftrightarrow S \cap U'$, which can change any point only by a vector of Λ . Hence $\text{Dif}(S \cap U) \equiv \text{Dif}(S \cap U') \pmod{\Lambda}$ as multi-sets with multiplicities respected by the bijection above.

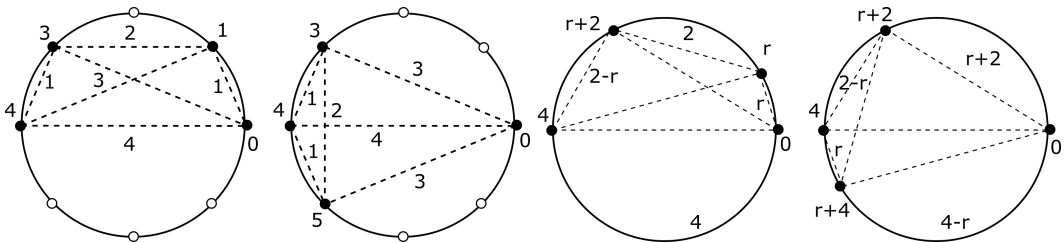
To determine if periodic sets $S, Q \subset \mathbb{R}^n$ are homometric by Definition 3, first we compute all $O(m^2)$ pairwise vector differences between points from the motifs $S \cap U$ and $Q \cap U$.

To check if these vector sets coincide, we could lexicographically order them in time $O(m^2 \log m)$, e.g. by using coordinates in the basis of the cell U . Then a single pass over $O(m^2)$ vector differences is enough to decide if $\text{Dif}(S) \equiv \text{Dif}(Q) \pmod{\Lambda}$. ◀

Patterson in [17, p. 197, Fig. 2] has suggested the 1D periodic sets $S = \{0, 1, 3, 4\} + 8\mathbb{Z}$ and $Q = \{0, 3, 4, 5\} + 8\mathbb{Z}$, see Fig. 3 and 4. Theorem 6 will justify why S, Q are non-isometric.



■ **Figure 3** Non-isometric homometric sets, see Definition ???. **Top:** $S(r) = \{0, r, r+2, 4\} + 8\mathbb{Z}$. **Bottom:** $Q(r) = \{0, r+2, 4, r+4\} + 8\mathbb{Z}$, where $0 < r \leq 1$ is a parameter. The simpler versions on the left hand side correspond to $r = 1$. The circular versions of these homometric sets are in Fig. 4.



■ **Figure 4 First two:** circular versions of the homometric sets S, Q in Fig. 3. Each circle splits into 8 equal arcs. The distances between points (shown outside the disk) are arc lengths (shown inside the disk). **Last two:** homometric sets $S(r) = \{0, r, r+2, 4\} + 8\mathbb{Z}$, $Q(r) = \{0, r+2, 4, r+4\} + 8\mathbb{Z}$, $0 < r < 2$. The distances between points shown outside the disk are arc lengths (inside the disk).

The vector differences of the 4-point motifs of the periodic sets S, Q in Fig. 3 differ:

S	0	1	3	4	Q	0	3	4	5
0	0	-1	-3	-4	0	0	-3	-4	-5
1	1	0	-2	-3	and 3	3	0	-1	-2
3	3	2	0	-1	4	4	1	0	-1
4	4	1	3	0	5	5	2	1	0

These signed distances coincide modulo 8 with infinite multiplicities: $\text{Dif}(S) \equiv \{0, 1, 2, 3, 4, 5, 6, 7\} \equiv \text{Dif}(Q) \pmod{8}$.

The above equivalence of vector differences modulo 8 gives rise to a bijection between all 16 elements of the matrices above, hence to a bijection between the differences multi-sets $D(S) \rightarrow D(Q)$, e.g. the difference $(8i + 1) - (8j + 4) = 8(i - j) - 3 \equiv 5 \pmod{8}$ in S can be bijectively mapped to the difference $(8i + 5) - 8j = 8(i - j) + 5$ in Q .

Fig. 4 shows a generic pair from the family of homometric sets $S(r), Q(r)$, where $r = 1$ is for the sets S, Q on the left. The mirror image of $S(r) = \{0, r, r + 2, 4\} + 8\mathbb{Z}$ under the reflection $t \mapsto 4 - t$ coincides with $S(2 - r) = \{0, 2 - r, 4 - r, 4\} + 8\mathbb{Z}$, so they are equivalent up to isometries including reflections. Similarly, $Q(r)$ and $Q(2 - r)$ are isometric by $t \mapsto -t$. To distinguish these sets up to isometries in section 5, we can assume that $0 < r \leq 1$.

5 Isometry invariance of Average Minimum Distances

This section introduces Average Minimum Distances in Definition 5 and proves their isometry invariance and continuity in Theorems 6, 10, respectively. If a lattice $\Lambda \subset \mathbb{R}^n$ contains the origin 0, then $\text{AMD}_k(\Lambda)$ is the distance from 0 to its k -th nearest neighbor in Λ , see Fig. 5.

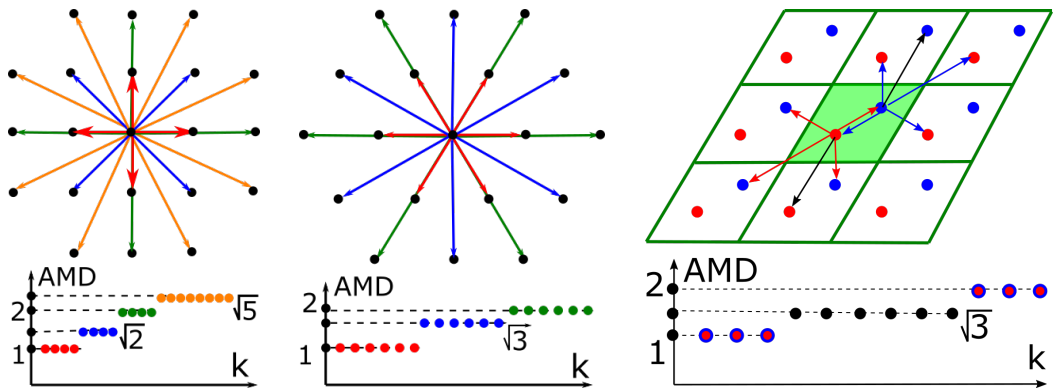


Figure 5 Left: in the square lattice, the k -th neighbors of the origin and corresponding AMD_k are shown in the same colour, e.g. $\text{AMD}_1 = \dots = \text{AMD}_4 = 1$ in red. **Middle:** in the hexagonal lattice, the first 6 values are in red: $\text{AMD}_1 = \dots = \text{AMD}_6 = 1$. **Right:** the motif of two points (red and blue) within a green unit cell has the first three equal distances: $\text{AMD}_1 = \text{AMD}_2 = \text{AMD}_3 = 1$.

► **Definition 5** (Average Minimum Distances AMD). Let a periodic set $S = \Lambda + M$ have points p_1, \dots, p_m in a primitive unit cell. For a fixed integer $k \geq 1$, consider the $m \times k$ matrix $D(S; k)$, whose i -th row consists of the ordered Euclidean distances $d_{i1} \leq \dots \leq d_{ik}$ measured from the point p_i to its first k nearest neighbors within the infinite set S . The Average Minimum Distance $\text{AMD}_k(S) = \frac{1}{m} \sum_{i=1}^m d_{ik}$ equals the average of the k -th column in the matrix $D(S; k)$. ■

Definition 5 is given for unlabeled points only for simplicity. If points have labels such as chemical elements, one can adapt AMD for labels as follows. For any two labels (say, O for oxygen and N for nitrogen) and i -th point p_i of type O, the matrix $D[O - N](S; k)$ has the i -th row of ordered distances from p_i to its k nearest neighbors of type N within S . Define $\text{AMD}[O - N](S; k)$ as the average of the k -th column of $D[O - N](S; k)$ over all points of type O in the motif of S .

In the top right picture of Fig. 5 the green unit cell has two points: one red and one blue (traditional colors for oxygen and nitrogen, respectively). Then $D[O - N] = \text{AMD}[O - N]$

consists of a single row of ordered distances from the red point to all its blue neighbors. The bottom right picture of Fig. 5 shows AMD values without taking labels into account.

For any finite set S of m points, $D(S; m-1)$ for the largest possible $k = m-1$ has all pairwise distances, but differs from the usual symmetric distance matrix of S due to the ordered distances in each row and the lexicographic order of all rows. This extra pointwise information distinguishes the 4-point sets in Fig. 2. The trapezium set T and kite set K in \mathbb{R}^2 can be represented by the points $(\pm 1, 1), (\pm 2, 0)$ and $(-2, 0), (-1, \pm 1), (2, 0)$, respectively.

Then $D(T; 3) = \begin{pmatrix} \sqrt{2} & 2 & \sqrt{10} \\ \sqrt{2} & 2 & \sqrt{10} \\ \sqrt{2} & \sqrt{10} & 4 \\ \sqrt{2} & \sqrt{10} & 4 \end{pmatrix}$ and $D(K; 3) = \begin{pmatrix} \sqrt{2} & \sqrt{2} & \sqrt{10} \\ \sqrt{2} & 2 & \sqrt{10} \\ \sqrt{2} & 2 & \sqrt{10} \\ \sqrt{10} & \sqrt{10} & 4 \end{pmatrix}$ are the matrices from Definition 5. The vectors $\text{AMD}(T) = (\sqrt{2}, 1 + \frac{\sqrt{10}}{2}, 2 + \frac{\sqrt{10}}{2})$ and $\text{AMD}(K) = (\frac{3\sqrt{2} + \sqrt{10}}{4}, 1 + \frac{\sqrt{2} + \sqrt{10}}{4}, 1 + \frac{3}{4}\sqrt{10})$ distinguish K, T up to isometry.

For a periodic set S , the index k can be chosen arbitrarily large, because Definition 5 looks for neighbors of motif points in the full infinite set S without restrictions to a unit cell or its finite extension. Hence increasing k only adds new larger distances without changing smaller ones. The homometric sets $S = \{0, 1, 3, 4\} + 8\mathbb{Z}$ and $Q = \{0, 3, 4, 5\} + 8\mathbb{Z}$ (both

with period 8) from Fig. 3 have $D(S; 3) = \begin{pmatrix} 1 & 2 & 3 \\ 1 & 2 & 3 \\ 1 & 3 & 4 \\ 1 & 3 & 4 \end{pmatrix}$ and $D(Q; 3) = \begin{pmatrix} 1 & 1 & 4 \\ 1 & 2 & 3 \\ 1 & 2 & 3 \\ 3 & 3 & 4 \end{pmatrix}$ with

the ordered motifs $M(S) = (1, 3, 0, 4)$ and $Q(S) = (4, 3, 5, 0)$, respectively. $D(S; 3)$ contains two pairs of identical rows, because $S = \{0, 1, 3, 4\} + 8\mathbb{Z}$ is symmetric with respect to the reflection $t \mapsto 4 - t \pmod{8}$. The similar reflection $t \mapsto -t \pmod{8}$ explains two identical rows in $D(Q; 3)$. Table 2 implies by Theorem 6 that the hard-to-distinguish sets $S(r), Q(r)$ in Fig. 4 are not isometric. The first column of $D(S(r); 3)$ contains the minimum distance r , which distinguishes $S(r)$ between each other for different $0 < r \leq 1$.

$D(S(r); 3)$	1st distance	2nd distance	3rd distance
$p_1 = 0$	$ 0 - r = r$	$ 0 - (2 + r) = 2 + r$	$ 0 - 4 = 4$
$p_2 = r$	$ r - 0 = r$	$ r - (2 + r) = 2$	$ r - 4 = 4 - r$
$p_3 = 2 + r$	$ (2 + r) - 4 = 2 - r$	$ (2 + r) - r = 2$	$ (2 + r) - 0 = 2 + r$
$p_4 = 4$	$ 4 - (2 + r) = 2 - r$	$ 4 - r = 4 - r$	$ 4 - 0 = 4$
$\text{AMD}_k(S(r))$	$\text{AMD}_1 = 1$	$\text{AMD}_2 = 2.5$	$\text{AMD}_3 = 3.5$

$D(Q(r); 3)$	1st distance	2nd distance	3rd distance
$p_1 = 0$	$ 0 - (2 + r) = 2 + r$	$ 0 - (r + 4 - 8) = 4 - r$	$ 0 - 4 = 4$
$p_2 = 2 + r$	$ (2 + r) - 4 = 2 - r$	$ (2 + r) - (4 + r) = 2$	$ (2 + r) - 0 = 2 + r$
$p_3 = 4$	$ 4 - (4 + r) = r$	$ 4 - (2 + r) = 2 - r$	$ 4 - 0 = 4$
$p_4 = 4 + r$	$ (4 + r) - 4 = r$	$ (4 + r) - (2 + r) = 2$	$ (4 + r) - 8 = 4 - r$
$\text{AMD}_k(Q(r))$	$\text{AMD}_1 = 1 + 0.5r$	$\text{AMD}_2 = 2.5 - 0.5r$	$\text{AMD}_3 = 3.5$

Table 2 The matrices $D(S; k)$ and average minimum distances from Definition 5 for the periodic sets $S(r) = \{0, r, r + 2, 4\} + 8\mathbb{Z}$, $Q(r) = \{0, r + 2, 4, r + 4\} + 8\mathbb{Z}$, $0 < r \leq 1$.

► **Theorem 6** (isometry invariance of AMD). *For any finite or periodic set $S \subset \mathbb{R}^n$, the Average Minimum Distance $\text{AMD}_k(S)$ from Definition 5 is an isometry invariant of S for any $k \geq 1$.* ■

Proof. For periodic sets, first we show that the unordered collections of rows of the matrix $D(S; k)$, and hence $\text{AMD}_k(S)$, is independent of a primitive unit cell. Let U, U' be primitive cells of a periodic set $S \subset \mathbb{R}^n$ with a lattice Λ . Any point $q \in S \cap U'$ can be translated along $\vec{v} \in \Lambda$ to a point $p \in S \cap U$ and vice versa. These translations establish a bijection between the motifs $S \cap U \leftrightarrow S \cap U'$ and preserve all distances. $D(S; k)$ is the same for both U, U' up to a permutation of rows .

Now we prove that $D(S; k)$, and hence $\text{AMD}_k(S)$, is preserved by any isometry $f : S \rightarrow Q$. Any primitive cell U of S is bijectively mapped by f to the unit cell $f(U)$ of Q , which should be also primitive. Indeed, if Q is preserved by a translation along a vector \vec{v} that doesn't have all integer coefficients in the basis of $f(U)$, then $S = f^{-1}(Q)$ is preserved by the translation along $f^{-1}(\vec{v})$, which also doesn't have all integer coefficients in the basis of U , i.e. U was non-primitive. Since both primitive cells U and $f(U)$ contain the same number of points from S and $Q = f(S)$, the isometry f gives a bijection between all motif points of S, Q .

For any (finite or periodic) sets S, Q , since the isometry f preserves distances, every list of ordered distances from any point $p_i \in S \cap U$ to its first k nearest neighbors in S coincides with the list of the ordered distances from $f(p_i)$ to its first k neighbors in Q . The matrices $D(S; k)$ and $D(Q; k)$ are identical up to permutations of rows, hence $\text{AMD}_k(S) = \text{AMD}_k(Q)$. ◀

6 Continuity of Average Minimum Distances under perturbations

To get a continuous isometry invariant, unit cell U in Definition 5 should be primitive. If U contains m points and we make one edge of U twice longer, the resulting non-primitive unit cell contains $2m$ points and the matrix $D(S; k)$ will be twice larger. A translated copy of any point $p_i \in U$ will have exactly the same ordered distances to its neighbors as p_i due to periodicity. After doubling U , every row is repeated twice in $D(S; k)$. The requirement of a primitive cell U makes $D(S; k)$ discontinuous similarly to the volume of U as in Fig. 2. One way to resolve the above discontinuity is Theorem 10 for AMD.

Since all atoms vibrate above the absolute zero temperature, the bottleneck distance d_B between periodic sets in Definition 7 naturally quantifies crystal similarities.

► **Definition 7** (packing radius $r(S)$ and bottleneck distance d_B). The *packing radius* $r(S)$ of a finite or periodic set S is the minimum half-distance between any points of S , or $r(S)$ is the maximum radius r to have disjoint open balls of radius r centered at all points of S . For a fixed bijection $g : S \rightarrow Q$ between finite or periodic sets $S, Q \subset \mathbb{R}^n$, the *maximum deviation* is the supremum $\sup_{a \in S} |a - g(a)|$ of Euclidean distances over all points in S . The *bottleneck distance* is $d_B(S, Q) = \inf_{g: S \rightarrow Q} \sup_{a \in S} |a - g(a)|$ is the infimum over all bijections $g : S \rightarrow Q$. ■

The key obstacle in a direct computation of the bottleneck distance d_B is the minimization over infinitely many bijections between infinite sets. Any reduction to a finite subset is hard to justify because of the discontinuity of a unit cell under perturbations [3]. Theorem 10 will justify that the isometry invariants AMD continuously quantify crystal similarities.

► **Lemma 8** (common lattice). Let periodic point sets $S, Q \subset \mathbb{R}^n$ have a bottleneck distance $d_B(S, Q) < r(Q)$, where $r(Q)$ is the packing radius. Then S, Q have a common lattice Λ with a unit cell U such that $S = \Lambda + (U \cap S)$, $Q = \Lambda + (U \cap Q)$. ■

Proof. Let $S = \Lambda(S) + (U(S) \cap S)$ and $Q = \Lambda(Q) + (U(Q) \cap Q)$, where $U(S), U(Q)$ are initial unit cells of S, Q and the lattices $\Lambda(S), \Lambda(Q)$ of S, Q contain the origin.

By shifting all points of S, Q (but not their lattices), we guarantee that S contains the origin 0 of \mathbb{R}^n . Assume by contradiction that the given periodic point sets S, Q have no common lattice. Then there is a vector $\vec{p} \in \Lambda(S)$ whose all integer multiples $k\vec{p} \notin \Lambda(Q)$ for $k \in \mathbb{Z} - 0$. Any such multiple $k\vec{p}$ can be translated by a vector $\vec{v}(k) \in \Lambda(Q)$ to the initial unit cell $U(Q)$ so that $\vec{q}(k) = k\vec{p} - \vec{v}(k) \in U(Q)$.

Since $U(Q)$ contains infinitely many points $\vec{q}(k)$, one can find a pair $\vec{q}(i), \vec{q}(j)$ at a distance less than $\delta = r(Q) - d_B(S, Q) > 0$. The formula $\vec{q}(k) \equiv k\vec{p} \pmod{\Lambda(Q)}$ implies that $\vec{q}(i+k(j-i)) \equiv (i+k(j-i))\vec{p} \pmod{\Lambda(Q)} \equiv \vec{q}(i) + k(\vec{q}(j) - \vec{q}(i)) \pmod{\Lambda(Q)}$.

If the point $\vec{q}(i) + k(\vec{q}(j) - \vec{q}(i))$ belongs to $U(Q)$, we get the equality $\vec{q}(i+k(j-i)) = \vec{q}(i) + k(\vec{q}(j) - \vec{q}(i))$. All these points over $k \in \mathbb{Z}$ lie on a straight line within $U(Q)$ and have the distance $|\vec{q}(j) - \vec{q}(i)| < \delta$ between successive points.

The closed balls with radius $d_B(S, Q)$ and centers at points in Q are at least 2δ away from each other. Then one of the points $\vec{q}(i+k(j-i))$ is more than $d_B(S, Q)$ away from Q . Hence the point $(i+k(j-i))\vec{p} \in S$ also has a distance more than $d_B(S, Q)$ from any point of Q , which contradicts Definition 7. \blacktriangleleft

► **Lemma 9** (perturbed distances). For some $\varepsilon > 0$, let $g : S \rightarrow Q$ be a bijection between finite or periodic sets such that $|a - g(a)| \leq \varepsilon$ for all $a \in S$. For any $i \geq 1$, let $a_i \in S$ and $b_i \in Q$ be the i -nearest neighbors of $a \in S$ and $b = g(a) \in Q$, respectively. Then the Euclidean distances from a, b to their i -th neighbors a_i, b_i are 2ε -close, i.e. $||a - a_i| - |b - b_i|| \leq 2\varepsilon$. \blacksquare

Proof. Translate the full set Q by the vector $a - g(a)$. So we assume that $a = g(a)$ and $|b - g(b)| < 2\varepsilon$ for all $b \in S$.

Assume by contradiction that the distance from a to its i -th neighbor b_i is less than $|a - a_i| - 2\varepsilon$. Then all first i neighbors b_1, \dots, b_i of a within Q belong to the open ball with the center a and the radius $|a - a_i| - 2\varepsilon$. Since the bijection g shifted every point b_1, \dots, b_i by at most 2ε , their preimages $g^{-1}(b_1), \dots, g^{-1}(b_i)$ belong to the open ball with the center $a = g(a)$ and the radius $|a - a_i|$. Then the i -th neighbor of a within S is among these i preimages. Hence the distance from a to its i -th nearest neighbor is strictly less than the required distance $|a - a_i|$. A similar contradiction is obtained from the assumption that the distance from a to its new i -th neighbor b_i is more than $|a - a_i| + 2\varepsilon$. \blacktriangleleft

The packing radius $r(S)$ and bottleneck distance d_B are introduced in Definition 7.

► **Theorem 10** (continuity of AMD under point perturbations). *Let finite or periodic sets S, Q satisfy $d_B(S, Q) < \frac{r(S)}{4}$. Then $|\text{AMD}_k(S) - \text{AMD}_k(Q)| \leq 2d_B(S, Q)$ for any $k \geq 1$.* \blacksquare

Proof. By Lemma 8 the sets S, Q have a common lattice Λ . Any primitive cell U of Λ is a unit cell of S, Q , i.e. $S = \Lambda + (S \cap U)$ and $Q = \Lambda + (Q \cap U)$. Since the bottleneck distance $\varepsilon = d_B(S, Q) < r(S)$, we can define a bijection g from every point $a \in S$ to its unique ε -closest neighbor $g(a) \in Q$.

If U is a non-primitive unit cell of S , the matrix $D(S; k)$ can be constructed as in Definition 5, but each row will be repeated $n(S) > 1$ times, where $n(S)$ is $\text{Vol}[U]$ divided by the volume of a primitive unit cell of S . The average $\text{AMD}_k(S)$ in the k -th column is independent of the factor $n(S) > 1$.

Since the above conclusions hold for Q instead of S , we now compare the matrices $D(S; k)$ and $D(Q; k)$ that are built on the same unit cell U and have equal sizes.

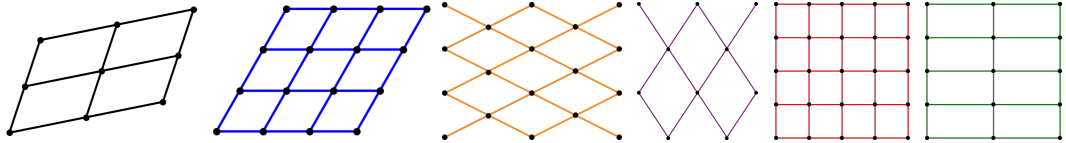
By Lemma 9 the corresponding elements of the matrices $D(S; k)$ and $D(Q; k)$ differ by at most 2ε , i.e. $|D_{ij}(S; k) - D_{ij}(Q; k)| \leq 2\varepsilon$. Then the average of the k -th column changes by at most 2ε , i.e. $|\text{AMD}_k(S) - \text{AMD}_k(Q)| \leq 2\varepsilon$. \blacktriangleleft

7 The asymptotic behaviour of the Average Minimum Distances

Theorem 14 explicitly describes the growth of AMD_k as $k \rightarrow +\infty$ for a wide class of sets including non-periodic. Briefly, any curve $\text{AMD}_k(S)$ approaches $c(S) \sqrt[k]{k}$, where the point packing coefficient $c(S)$ is related to the single-value density of a periodic crystal. Asymptotic Theorem 14 will hold for a wide class of (U, m) -sets, which may not be periodic.

The volume of the unit ball in \mathbb{R}^n is $V_n = \frac{\pi^{n/2}}{\Gamma(\frac{n}{2} + 1)}$, where Γ denotes Euler's Gamma function, e.g. $\Gamma(m) = (m-1)!$ and $\Gamma(\frac{m}{2} + 1) = \sqrt{\pi}(m - \frac{1}{2})(m - \frac{3}{2}) \cdots \frac{1}{2}$ for any integer m .

► **Definition 11** ($\text{AMD}_k(S; U)$ and the point packing coefficient $c(S)$ for (U, m) -sets S). Let U be a unit cell generating a lattice $\Lambda \subset \mathbb{R}^n$. For a fixed $m \geq 1$, a set $S \subset \mathbb{R}^n$ is a (U, m) -set if $S \cap (U + \vec{v})$ consists of m points for any $\vec{v} \in \Lambda$. For any point $p \in S \cap U$, let $d_k(S; p)$ be the distance from p to its k -th nearest neighbor in S . The *average minimum distance* is $\text{AMD}_k(S; U) = \frac{1}{m} \sum_{p \in S \cap U} d_k(S; p)$. The *point packing coefficient* is $c(S) = \sqrt[m]{\frac{\text{Vol}[U]}{mV_n}}$. \blacksquare



► **Figure 6** 1st: a generic black lattice Λ_1 with the basis $(1.25, 0.25), (0.25, 0.75)$ and $c(\Lambda_1) = \sqrt{\frac{7}{8\pi}} \approx 0.525$. 2nd: the blue hexagonal lattice Λ_2 with the basis $(1, 0), (1/2, \sqrt{3}/2)$ and $c(\Lambda_2) = \sqrt{\frac{\sqrt{3}}{2\pi}} \approx 0.528$. 3rd: the orange rhombic lattice Λ_3 with the basis $(1, 0.5), (1, -0.5)$ and $c(\Lambda_3) = \sqrt{\frac{1}{\pi}} \approx 0.564$. 4th: the purple rhombic lattice Λ_4 with the basis $(1, 1.5), (1, -1.5)$ and $c(\Lambda_4) = \sqrt{\frac{3}{\pi}} \approx 0.977$. 5th: the red square lattice Λ_5 with the basis $(1, 0), (0, 1)$ and $c(\Lambda_5) = \sqrt{\frac{1}{\pi}} \approx 0.564$. 6th: the green rectangular lattice Λ_6 with the basis $(2, 0), (0, 1)$ and $c(\Lambda_6) = \sqrt{\frac{2}{\pi}} \approx 0.798$.

A typical example of a (U, m) -set is a non-periodic perturbation of a periodic set $S = \Lambda + M$, where a lattice Λ is generated by a unit cell U and a motif M consists of m points. Since S may not be periodic, $\text{AMD}_k(S; U + \vec{v})$ can depend on a shift vector $\vec{v} \in \Lambda$. Even if S is periodic, a unit cell U in Definition 11 can be non-primitive, but $\frac{\text{Vol}[U]}{m}$ is independent of a choice of a unit cell U . Hence the point packing coefficient $c(S)$ is an isometry invariant, also for a (U, m) -set S , because any shifted cell $U + \vec{v}$ contains the same number m of points from S . If all points have the weight V_n of the unit ball in \mathbb{R}^n , then $(c(S))^n$ is inversely proportional to the classical density of S . Fig. 6 shows six lattices Λ_i with $c(\Lambda_i)$.

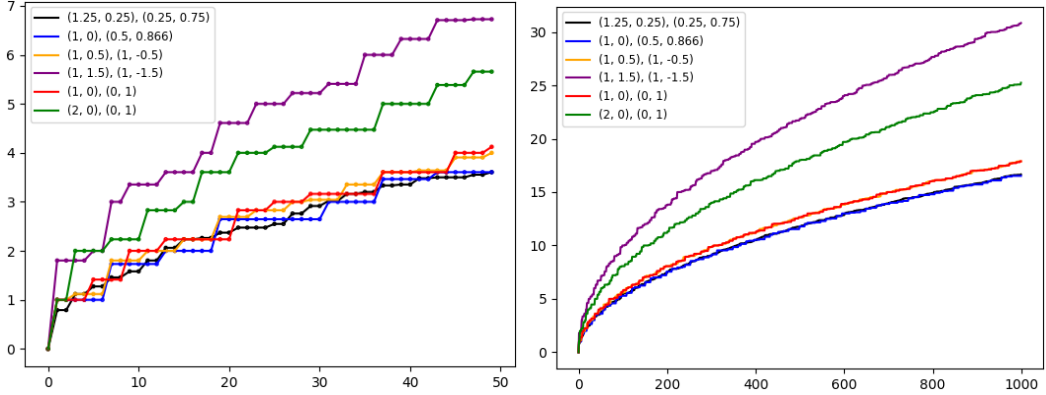


Figure 7 **Left:** AMD_k up to $k = 50$ for the 2D lattices in Fig. 6. **Right:** AMD_k extended up to $k = 1000$. When $k \rightarrow +\infty$ the orange and red graphs become very close as well as the blue and black graphs as explained by Theorem 14, see clearer differences for smaller k on the left.

The coefficients $c(\Lambda_i)$ in Fig. 6 explain the AMD curves in Fig. 7 due to Theorem 14. The diameter of a unit cell U is $d = \sup_{a, b \in U} |\vec{a} - \vec{b}|$. Lemmas 12 and 13 will prove Theorem 14.

► **Lemma 12** (bounds on points within a ball). Let $S \subset \mathbb{R}^n$ be any (U, m) -set with a unit cell U , which generates a lattice Λ and has a diameter d . For any point $p \in S \cap U$ and a radius r ,

consider the *lower* union $U'(p; r) = \bigcup \{(U + \vec{v}) \text{ such that } \vec{v} \in \Lambda, (U + \vec{v}) \subset \bar{B}(p; r)\}$

and the *upper* union $U''(p; r) = \bigcup \{(U + \vec{v}) \text{ such that } \vec{v} \in \Lambda, (U + \vec{v}) \cap \bar{B}(p; r) \neq \emptyset\}$.

Then the number of points from S in the closed ball $\bar{B}(p; r)$ with center p and radius r has the bounds $\left(\frac{r-d}{c(S)}\right)^n \leq m \frac{\text{Vol}[U'(p; r)]}{\text{Vol}[U]} \leq |S \cap \bar{B}(p; r)| \leq m \frac{\text{Vol}[U''(p; r)]}{\text{Vol}[U]} \leq \left(\frac{r+d}{c(S)}\right)^n$. ■

Proof. Intersect the three regions $U'(p; r) \subset \bar{B}(p; r) \subset U''(p; r)$ with S in \mathbb{R}^n and count the numbers of resulting points: $|S \cap U'(p; r)| \leq |S \cap \bar{B}(p; r)| \leq |S \cap U''(p; r)|$.

The union $U'(p; r)$ consists of $\frac{\text{Vol}[U'(p; r)]}{\text{Vol}[U]}$ cells, which all have the same volume $\text{Vol}[U]$. Since $|S \cap U| = m$, we get $|S \cap U'(p; r)| = m \frac{\text{Vol}[U'(p; r)]}{\text{Vol}[U]}$. Similarly we count the points in the upper union: $|S \cap U''(p; r)| = m \frac{\text{Vol}[U''(p; r)]}{\text{Vol}[U]}$. The bounds of $|S \cap \bar{B}(p; r)|$ become

$$m \frac{\text{Vol}[U'(p; r)]}{\text{Vol}[U]} \leq |S \cap \bar{B}(p; r)| \leq m \frac{\text{Vol}[U''(p; r)]}{\text{Vol}[U]},$$

$$\text{Vol}[U'(p; r)] \leq \frac{\text{Vol}[U]}{m} |S \cap \bar{B}(p; r)| \leq \text{Vol}[U''(p; r)].$$

For the diameter d of the unit cell U , the smaller ball $\bar{B}(p; r-d)$ is completely contained within the lower union $U'(p; r)$. Indeed, if $|\vec{q} - \vec{p}| \leq r-d$, then $\vec{q} \in U + \vec{v}$ for some $\vec{v} \in \Lambda$. Then $(U + \vec{v})$ is covered by the ball $\bar{B}(\vec{q}; d)$, hence by $\bar{B}(p; r)$ due to the triangle inequality.

The inclusion $\bar{B}(p; r-d) \subset U'(p; r)$ implies the lower bound for the volumes: $V_n(r-d)^n = \text{Vol}[\bar{B}(p; r-d)] \leq \text{Vol}[U'(p; r)]$, where V_n is the volume of the unit ball in \mathbb{R}^n . The similar

inclusion $U''(p; r) \subset \bar{B}(p; r + d)$ gives $\text{Vol}[U''(p; r)] \leq \text{Vol}[\bar{B}(p; r + d)] = V_n(r + d)^n$. Then

$$V_n(r - d)^n \leq \frac{\text{Vol}[U]}{m} |S \cap B(p; r)| \leq V_n(r + d)^n,$$

$$\frac{mV_n}{\text{Vol}[U]}(r - d)^n \leq |S \cap B(p; r)| \leq \frac{mV_n}{\text{Vol}[U]}(r + d)^n,$$

which is equivalent to the required inequality with $c(S) = \sqrt[n]{\frac{\text{Vol}[U]}{mV_n}}$. \blacktriangleleft

► **Lemma 13** (distance bounds). Let $S \subset \mathbb{R}^n$ be any (U, m) -set with a unit cell U of diameter d . For any point $p \in S \cap U$, let $d_k(S; p)$ be the distance from p to its k -th nearest neighbor in S . Then $c(S) \sqrt[n]{k} - d < d_k(S; p) \leq c(S) \sqrt[n]{k} + d$ for any $k \geq 1$. \blacksquare

Proof. The closed ball $\bar{B}(p; r)$ of radius $r = d_k(S; p)$ has more than k points (including p) from S . The upper bound of Lemma 12 for $r = d_k(S; p)$ implies that $k < |S \cap \bar{B}(p; r)| \leq \frac{(r + d)^n}{(c(S))^n}$.

Taking the n -th root of both sides, we get $\sqrt[n]{k} < \frac{r + d}{c(S)}$, $r = d_k(S; p) > c(S) \sqrt[n]{k} - d$.

For any smaller radius $r < d_k(S; p)$, the closed ball $\bar{B}(p; r)$ contains at most k points (including p) from S . The lower bound of Lemma 12 for any $r < d_k(S; p)$ implies that $\frac{(r - d)^n}{c(S)^n} \leq |S \cap \bar{B}(p; r)| \leq k$. Since $\frac{(r - d)^n}{c(S)^n} \leq k$ holds for the constant upper bound k and any radius $r < d_k(S; p)$, the same inequality holds for the radius $r = d_k(S; p)$.

Similarly to the upper bound above, we get $\frac{r - d}{c(S)} \leq \sqrt[n]{k}$, $r = d_k(S; p) \leq c(S) \sqrt[n]{k} + d$.

Combine the two bounds above: $c(S) \sqrt[n]{k} - d < d_k(S; p) \leq c(S) \sqrt[n]{k} + d$. \blacktriangleleft

► **Theorem 14** (asymptotic behaviour of AMD). For any (U, m) -set $S \subset \mathbb{R}^n$ from Definition 11, we have $|\text{AMD}_k(S; U) - c(S) \sqrt[n]{k}| \leq d$ for any $k \geq 1$ and $\lim_{k \rightarrow +\infty} \frac{\text{AMD}_k(S; U)}{\sqrt[n]{k}} = c(S)$. \blacksquare

Proof of Theorem 14. Averaging the bounds of Lemma 13 over all points $p \in S \cap U$, we get the required bounds: $c(S) \sqrt[n]{k} - d < \text{AMD}_k(S; U) = \frac{1}{m} \sum_{p \in S \cap U} d_k(S; p) \leq c(S) \sqrt[n]{k} + d$, which imply that $|\text{AMD}_k(S; U) - c(S) \sqrt[n]{k}| \leq d$ for $k \geq 1$, hence $\lim_{k \rightarrow +\infty} \frac{\text{AMD}_k(S; U)}{\sqrt[n]{k}} = c(S)$. \blacktriangleleft

8 A fast AMD algorithm and experiments on large crystal datasets

This section describes the algorithm to compute the new isometry invariants PDD and AMD from Definition 5 and then discusses experiments on real and simulated crystals.

The input for computing the new invariants PDD and AMD is a periodic point set S given by (parameters of) its unit cell U and coordinates of m motif points in the basis of U . For any crystal, this information is contained in its Crystallographic Information File (CIF).

The length k of the AMD vector $(\text{AMD}_1, \dots, \text{AMD}_k)$ is independent of a crystal. Increasing k adds more components to the AMD vector without changing the previous ones. Due to Theorem 14, if periodic sets have the same point packing coefficient, a beginning of the AMD vector can be enough to distinguish them up to isometry, see the left picture of Fig. 7.

► **Proposition 15** (a fast algorithm for AMD). Let a periodic set $S \subset \mathbb{R}^n$ have m points in a unit cell U . For a fixed dimension n , the average minimum distances $\text{AMD}_i(S)$ for $i = 1, \dots, k$ can be computed in a time $O(\nu(S; n)km \log(km))$, where $\nu(S; n)$ is a function independent of k, m . ■

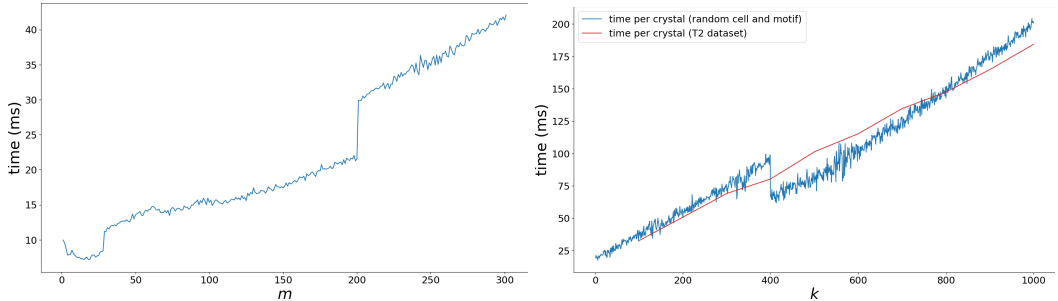
Proof. Let the origin 0 be in the center of the unit cell U , which generates a lattice Λ . If d is the diameter of U , any point $p \in M = S \cap U$ is covered by the closed ball $\bar{B}(0, 0.5d)$.

By Lemma 13 all k neighbors of p are covered by the ball $\bar{B}(0; r)$ of radius $r = c(S) \sqrt[n]{k} + 1.5d$. To generate all Λ -translates of M within $\bar{B}(0; r)$, we gradually extend U in spherical layers by adding more distant shifted cells until we get the upper union $U''(0; r) \supset \bar{B}(0; r)$. By Lemma 12 the union $U''(0; r)$ includes all k neighbors of motif points and has at most

$$\mu = m \frac{\text{Vol}[U''(0; r)]}{\text{Vol}[U]} \leq \left(\frac{c(S) \sqrt[n]{k} + 2.5d}{c(S)} \right)^n = \left(\sqrt[n]{k} + \frac{2.5d}{c(S)} \right)^n = O(f(S; n)k) \text{ points, where}$$

$f(S; n)$ denotes a suitable function that is independent of $k \rightarrow +\infty$ for a fixed dimension n . We build a balanced n -d tree [7] on μ points above in time $O(n\mu \log \mu)$. For each $p \in M$, all k neighbors of p can be found and ordered by distances to p in time $O(\mu \log \mu)$. By Definition 5 we lexicographically sort m lists of ordered distances in time $O(km \log m)$, because a comparison of any two ordered lists of length k takes $O(k)$ time. The ordered lists are the rows of $\text{PDD}(S; k)$. All $\text{AMD}_i(S)$ are found in time $O(km)$. The total time is $O((m+n)\mu \log \mu + km \log m) = O(\nu(S; n)km \log(km))$, where ν is independent of k, m . ◀

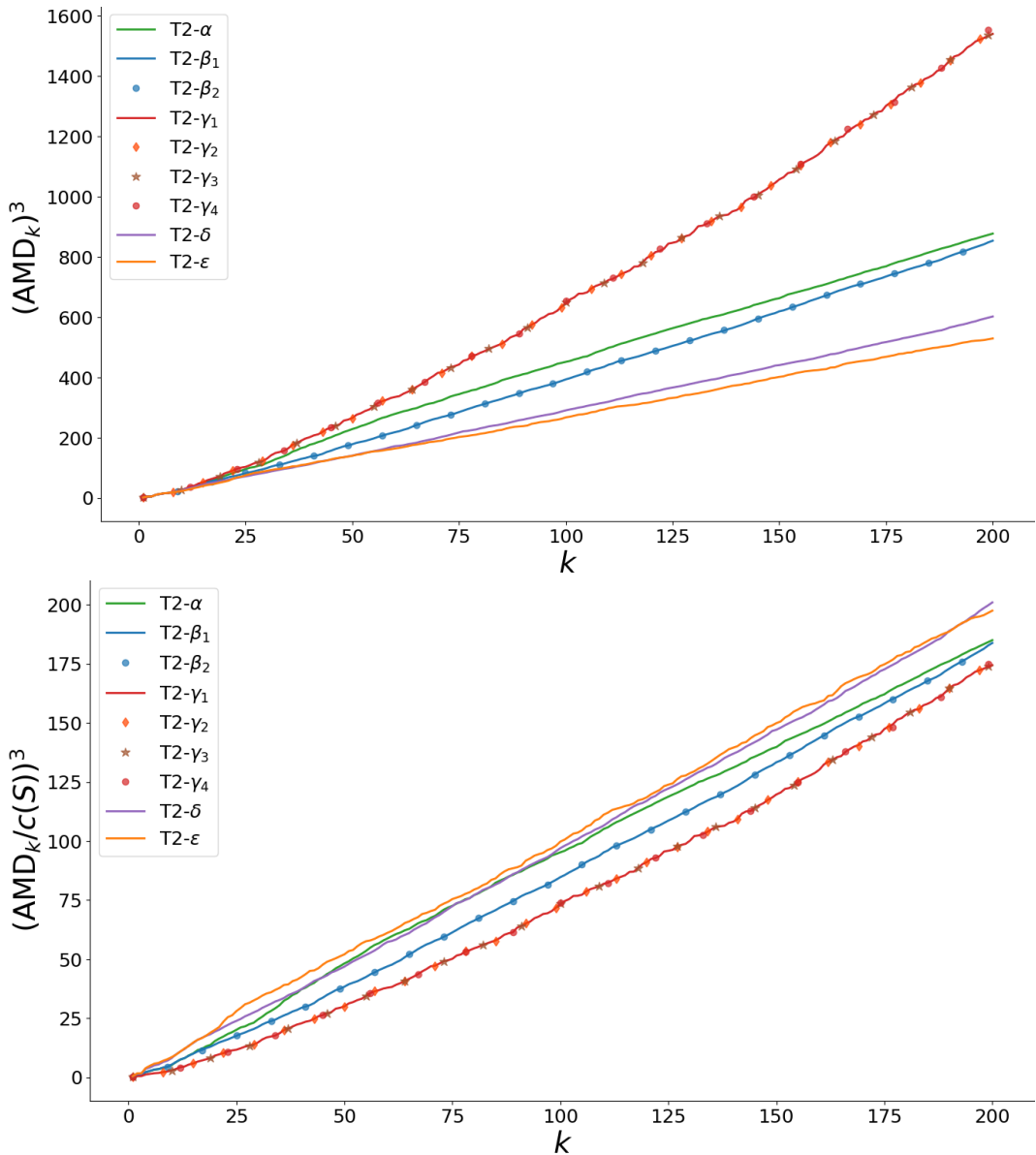
Fig. 8 illustrates the near linear running time as expected by Proposition 15. A few drops and jumps are explained in section B by generating extra layers of cells depending on $\frac{k}{m}$.



► **Figure 8** The blue curves show the AMD time in milliseconds averaged over 3000 sets whose points are randomly generated in unit cells with random edge-lengths in $[1, 2]$ and angles in $[\frac{\pi}{3}, \frac{2\pi}{3}]$. **Left:** AMDs up to $k = 200$. **Right:** the blue curve for $m = 400$, the red curve for 5679 T2 crystals.

The experiments are based on our earlier paper [18], which reported the experimental crystals T2- α , T2- β , T2- γ , T2- δ , see details in appendix B. Actually, eight versions were synthesized at different temperatures and deposited in the Cambridge Structural Database (CSD), the world's largest collection of more than 1M known materials. We use the following short notations and quote the CSD references in brackets: T2- α (NAVXUG), T2- β_1 (DEBXIT05), T2- β_2 (DEBXIT06), T2- γ_1 (DEBXIT01), T2- γ_2 (DEBXIT02), T2- γ_3 (DEBXIT03), T2- γ_4 (DEBXIT04), T2- δ (SEMDIA), T2- ε (synthesized later, to be deposited soon).

Fig. 9 shows the transformed AMD curves for the nine experimental T2 crystals above. The linear behavior of $(\text{AMD}_k(S))^3$ in the top diagram is explained by Theorem 14 and the



■ **Figure 9** Transformed AMDs for the experimental crystals with coefficients $c(S)$ from Table 3.

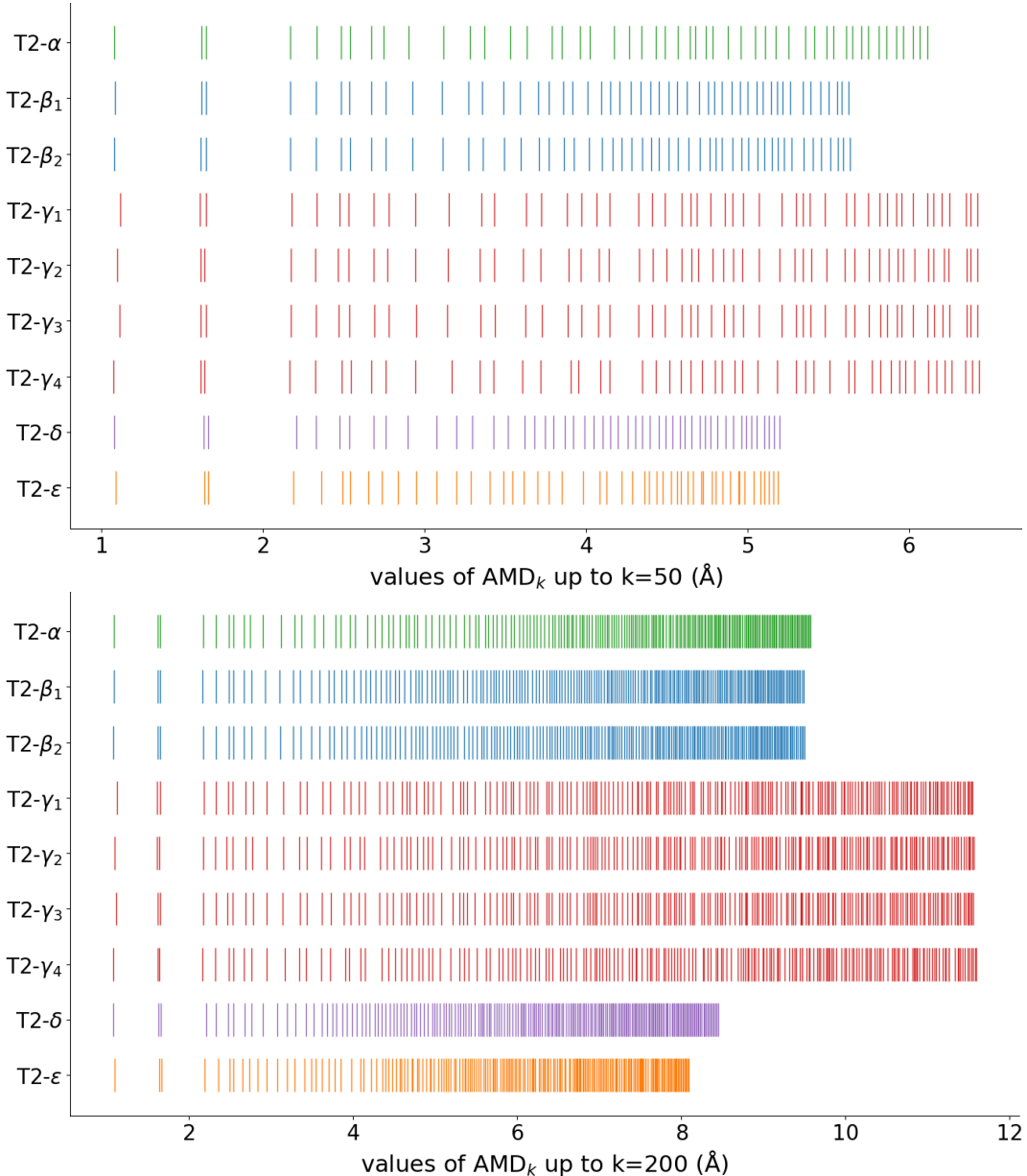
point packing coefficient $c(S)$ in Table 3. The five families T2- α , T2- β , T2- γ , T2- δ , T2- ϵ are visible even after the normalization by $c(S)$ in $\left(\frac{\text{AMD}_k(S)}{c(S)}\right)^3$, see *amdigrams* in Fig. 10.

Fig. 11 shows the dendrogram obtained by the L_∞ -distance, which is more stable with respect to the length k of AMD vectors than Euclidean L_2 due to Theorem 14. This dendrogram automatically identifies closest simulated crystals that were manually matched to experimental ones by a search through dozens of crystals that have close density values.



real T2 crystal	T2- α	T2- β_1	T2- β_2	T2- γ_1	T2- γ_2	T2- γ_3	T2- γ_4	T2- δ	T2- ϵ
density ρ (g/cm ³)	0.768	0.784	0.782	0.412	0.412	0.412	0.410	1.215	1.359
$c(S)$, Definition 11	1.680	1.668	1.669	2.067	2.067	2.067	2.071	1.441	1.389

■ **Table 3** The point packing coefficient $c(S)$ is roughly inversely proportional to the physical density ρ defined as the total weight of atoms within a unit cell divided by the unit cell volume.



■ **Figure 10** $AMD^{(k)}(S)$ of the nine T2 experimental crystals from Table 3 consist of vertical bars drawn at the values AMD_1, \dots, AMD_k on the horizontal axis, $1\text{Å} = 10^{-10}\text{m}$.

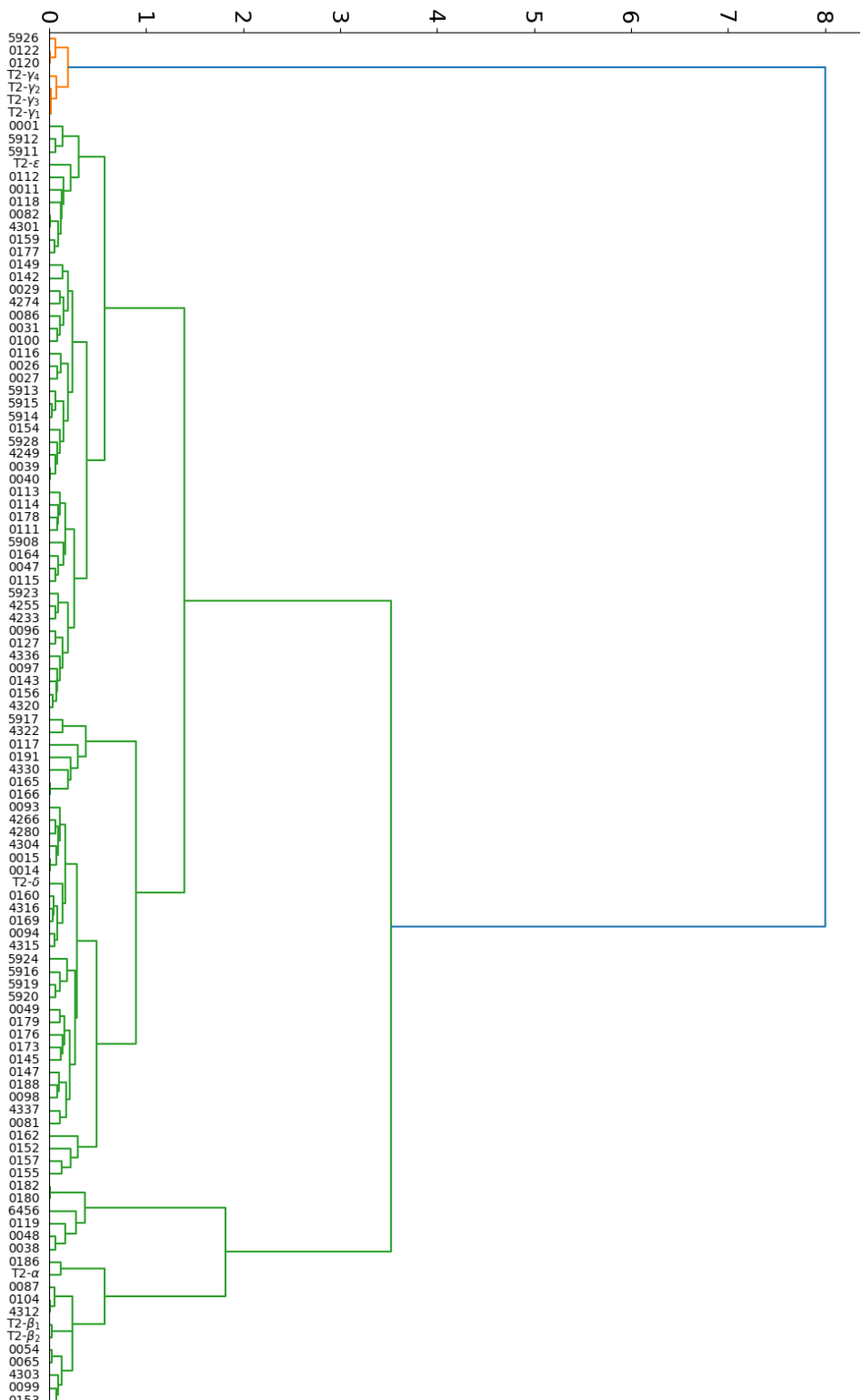


Figure 11 Complete-linkage clustering by the L_∞ distance on $(AMD_1, \dots, AMD_{1000})$ of T2 crystals: nine experimental and 100 (of 5679) simulated crystals with lowest energies, see [18].

9 Completeness for generic finite sets up to isometry and a discussion

The isometry classification of periodic point sets is motivated by important applications in materials discovery. Crystal Structure Prediction systematically over-predicts crystals by several orders of magnitudes. A 12-week optimization of 2M almost random structures on a supercomputer predicted 5679, but only five crystals were experimentally synthesized [18]. The key obstacle is the absence of efficient tools to filter out on the fly nearly identical structures obtained as approximations to the same local minimum of an energy function.

In addition to the homometric sets in Fig. 4, the invariant AMD_2 easily distinguishes another challenging pair S_{32}, Q_{32} from [9, Example 5.2], see details in [4, Example 7].

$$S_{32} = \{0, 7, 8, 9, 12, 15, 17, 18, 19, 20, 21, 22, 26, 27, 29, 30\} + 32\mathbb{Z},$$

$$Q_{32} = \{0, 1, 8, 9, 10, 12, 13, 15, 18, 19, 20, 21, 22, 23, 27, 30\} + 32\mathbb{Z}.$$

The final result below complements the isometry detection algorithm [2, Theorem 1] by justifying that the PDD matrix uniquely identifies an isometry type of any generic finite set.

► **Proposition 16** (completeness for generic finite sets). Let a finite set $S \subset \mathbb{R}^n$ consist of m points such that all pairwise distances between all points of S are distinct. *Lexicographically* order the rows of the matrix $D(S; m - 1)$ from Definition 5 as follows. A row (d_{i1}, \dots, d_{ik}) is *smaller* than (d_{j1}, \dots, d_{jk}) if the first (possibly none) distances coincide: $d_{i1} = d_{j1}, \dots, d_{il} = d_{jl}$ for some $l \in \{1, \dots, k - 1\}$ and the next $(l + 1)$ -st distances satisfy $d_{i,l+1} < d_{j,l+1}$. Then S can be uniquely reconstructed from $D(S; m - 1)$ up to isometry of \mathbb{R}^n . ■

Proof. Since the distances between all m points of $S \subset \mathbb{R}^n$ are distinct, every distance appears in the matrix $D(S; m - 1)$ exactly twice, once as the distance from a point p_i to its neighbor p_j , and once more as the distance from p_j to p_i , though these equal entries are not symmetric. We will convert $D(S; m - 1)$ into the distance matrix $D(S)$ as follows. Let $d_1 < d_2 < \dots < d_{m-1}$ be all distances from the first point $p_1 \in S$ to all $m - 1$ others.

Each distance d_i from the first row of $D(S; m - 1)$ appears exactly once more in another (say, i' -th) row of $D(S; m - 1)$. Then d_i is the distance between the points p_1 and $p_{i'}$ numbered as the i' -th row. The map of indices $i \mapsto i'$ is a permutation of $\{2, \dots, m\}$. We set $D_{11} = 0$ and $D_{1,i'} = d_i$ for each $i = 2, \dots, m$. Then we similarly permute indices in the 2nd row of $D(S; m - 1)$, starting from the 3rd index due to the symmetry of $D(S)$, and so on. The full distance matrix $D(S)$ uniquely determines a set with ordered points $S \subset \mathbb{R}^n$ modulo isometries by the classical multi-dimensional scaling in [14, Section 8.5.1]. ◀

The complementary work [9] introduces the density functions, which are also continuous isometric invariants of periodic sets, but don't distinguish the periodic sets $U \pm V + 15\mathbb{Z}$ for $U = \{0, 4, 9\}$ and $V = \{0, 1, 3\}$, see the beginning of section 5 [9]. The simple computation in [4, Example 6] shows that the above sets are distinguished by AMD_3 , hence AMDs are stronger than density functions in this case. Another strength of AMD is the clear interpretability in terms of distances and the asymptotic behavior in Theorem 14. The practical strength of AMDs is the fast time in Fig. 8, e.g. about 17 min up to $k = 1000$ for 5679 crystals on a standard desktop, as expected by Proposition 15.

Two AMD implementations [19, 15] produce identical results. We thank the authors of [9] and Janos Pach for fruitful discussions and all reviewers in advance for helpful suggestions.

References

- 1 Private communication with Larry Andrews. URL: <http://ronininstitute.org/research-scholars/larry-andrews>.
- 2 Helmut Alt, Kurt Mehlhorn, Hubert Wagener, and Emo Welzl. Congruence, similarity, and symmetries of geometric objects. *Discrete & Computational Geometry*, 3:237–256, 1988.
- 3 LC Andrews, HJ Bernstein, and GA Pelletier. A perturbation stable cell comparison technique. *Acta Crystallographica Section A*, 36(2):248–252, 1980.
- 4 Olga Anosova and Vitaliy Kurlin. Introduction to periodic geometry and topology. *arXiv:2103.02749*, 2021.
- 5 Olga Anosova and Vitaliy Kurlin. An isometry classification of periodic point sets. In *Proceedings of Discrete Geometry and Mathematical Morphology*, 2021.
- 6 M. Boutin and G. Kemper. On reconstructing n-point configurations from the distribution of distances or areas. *Advances in Applied Mathematics*, 32(4):709–735, 2004.
- 7 Russell A. Brown. Building a balanced k-d tree in $o(kn \log n)$ time. *J. Computer Graphics Techniques*, 4(1):50–68, 2015.
- 8 J. Chisholm and S. Motherwell. Compack: a program for identifying crystal structure similarity using distances. *J. Applied Crystallography*, 38(1):228–231, 2005.
- 9 Herbert Edelsbrunner, Teresa Heiss, Vitaliy Kurlin, Philip Smith, and Mathijs Wintraecken. The density fingerprint of a periodic point set. In *Proceedings of SoCG*, 2021.
- 10 J Franklin. Ambiguities in the x-ray analysis of crystal structures. *Acta Cryst. A*, 30:698–702, 1974.
- 11 T Hahn, U Shmueli, and J Arthur. *Internat. tables for crystallography*, volume 1. 1983.
- 12 Lauri Himanen, Marc OJ Jäger, Eiaki V Morooka, Filippo Federici Canova, Yashasvi S Ranawat, David Z Gao, Patrick Rinke, and Adam S Foster. Dscribe: Library of descriptors for machine learning in materials science. *Computer Physics Communications*, 247:106949, 2020.
- 13 Heuna Kim and Günter Rote. Congruence testing of point sets in 4 dimensions. *arXiv:1603.07269*, 2016.
- 14 Leo Liberti and Carlile Lavor. *Euclidean distance geometry: an introduction*. Springer, 2017.
- 15 M Mosca. Average Minimum Distances in C++. URL: <https://github.com/mmosca/AMD>.
- 16 Marco Mosca and Vitaliy Kurlin. Voronoi-based similarity distances between arbitrary crystal lattices. *Crystal Research and Technology*, 55(5):1900197, 2020.
- 17 A Patterson. Ambiguities in the x-ray analysis of crystal structures. *Phys. Rev.*, 65:195, 1944.
- 18 Angeles Pulido, Linjiang Chen, Tomasz Kaczorowski, Daniel Holden, M Little, Samantha Chong, Benjamin Slater, D McMahon, Baltasar Bonillo, C Stackhouse, A Stephenson, C Kane, R Clowes, Tom Hasell, Andrew Cooper, and Graeme Day. Functional materials discovery using energy–structure–function maps. *Nature*, 543:657–664, 2017.
- 19 D Widdowson. Average Min. Distances in Python. URL: <https://github.com/dwiddo/AMD>.
- 20 B. Zhilinskii. *Introduction to lattice geometry through group action*. EDP sciences, 2016.

A Background on isometries and isometry invariants

► **Definition 17** (isometries). An *isometry* of \mathbb{R}^n is any map $f : \mathbb{R}^n \rightarrow \mathbb{R}^n$ that preserves the Euclidean distance, i.e. $|pq| = |f(p)f(q)|$ for any points $p, q \in \mathbb{R}^n$. If f also preserves the *orientation*, i.e. the matrix whose columns are images under f of the standard basis vectors $\vec{e}_1, \dots, \vec{e}_n$ has a positive determinant, then f can be called a *rigid motion*, because f is included into a continuous family of isometries $f_\lambda : \mathbb{R}^n \rightarrow \mathbb{R}^n$, $\lambda \in [0, 1]$, where $f_1 = f$ and f_0 is the identity map $f_0(p) = p$ for any $p \in \mathbb{R}^n$. ■

Any isometry of \mathbb{R}^n can be decomposed into at most $n + 1$ reflections over hyperspaces, hence is bijective and can be inverted. A composition of isometries is also an isometry, which defines the operation in the group $\text{Iso}(\mathbb{R}^n)$ of all isometries in \mathbb{R}^n . Rigid motions

are orientation-preserving isometries and form the smaller subgroup $\text{Iso}^+(\mathbb{R}^n) \subset \text{Iso}(\mathbb{R}^n)$. Examples in \mathbb{R}^3 are translations by vectors and rotations around straight lines. It suffices to classify only up to general isometries, because if we know that two point sets S, Q are isometric, one can easily check if possible isometries $S \rightarrow Q$ preserve an orientation.

For any $n \times n$ matrix A , recall that A^T denotes the *transpose* matrix with elements $A_{ij}^T = A_{ji}$, $i, j = 1, \dots, n$. A matrix A is *orthogonal* if the inverse matrix A^{-1} equals the transpose A^T . Orthogonality of a matrix A means that $\vec{v} \mapsto A\vec{v}$ maps any orthonormal basis to another orthonormal basis. All orthogonal matrices A have the determinant $\det A = \pm 1$. If $\det A = 1$, then the map $\vec{v} \mapsto A\vec{v}$ preserves an orientation of \mathbb{R}^n .

All orthogonal matrices A with $\det A = 1$ form the special orthogonal group $\text{SO}(\mathbb{R}^n)$, where the operation is the matrix multiplication. The group $\text{SO}(\mathbb{R}^2)$ consists of rotations about the origin in the plane. The group $\text{SO}(\mathbb{R}^3)$ consists of rotations about axes passing through the origin in \mathbb{R}^3 . In general, $\text{SO}(\mathbb{R}^n)$ consists of all isometries from $\text{Iso}^+(\mathbb{R}^n)$ that preserve the origin. Any objects should be classified by invariants that are independent of a given representation of an object. Many machine learning algorithms struggle when features or descriptors include non-invariants of crystals, e.g. parameters of an ambiguous unit cell or atomic coordinates in an arbitrary basis.

► **Definition 18** (isometry invariant). An *isometry class* of sets is a collection of all sets that are isometric to each other, i.e. any sets S, Q from the same class are related by an isometry $S \rightarrow Q$. An *isometry invariant* is a function I that maps all sets of a certain type, e.g. all periodic sets, to a simpler space (e.g. numbers, matrices) so that $I(S) = I(Q)$ for any isometric sets S, Q . An invariant I is called *complete* if the converse is also true: if $I(S) = I(Q)$, then the sets S, Q are isometric. ■

B Applications of AMD invariants to Crystal Structure Prediction

All experiments were run on a modest desktop with Intel Core i5-4460 @ 3.20 GHz, 4 cores, RAM 16GB DDR3 @ 1333 MHz. Fig. 12 shows that occasional drops in the AMD running time correspond to the values of k/m when the algorithm from Proposition 15 generates new spherical 'layers' of unit cells containing more points obtained by translations from all motif points in an initial unit cell. Larger n -d trees allow faster queries for nearest neighbors.

The traditional approach to compare crystals is to reduce a basis of a lattice, e.g. to Niggli's reduced cell [11, section 9.3]. For over 40 years, Niggli's reduced cell has been known to be unstable under vibrations [3], which are always present above the absolute zero temperature. So many distant representations { crystal = lattice + motif } may define nearly identical crystals. Hence reduced cells are not practically used in pharmaceutical research.

The motivation for new continuous invariants is the 'embarrassment of over-prediction'. Modern tools of Crystal Structure Prediction (CSP) predict thousands of simulated crystals, though very few of them can be experimentally synthesized. The CSP run by supercomputers starts from millions of almost random arrangements of atoms or molecules and minimizes a complicated energy function. Lower energy values indicate that crystals will remain stable as solid materials, i.e. will not disintegrate. This energy has no closed expression due to the dependence on infinitely many interactions between all atoms within a periodic crystal.

A typical CSP software outputs thousands of approximate local minima of this energy, i.e. simulated crystals whose local perturbations are unlikely to produce more stable arrangements. Simulated crystals can be visualized by the energy-vs-density *landscape* representing each

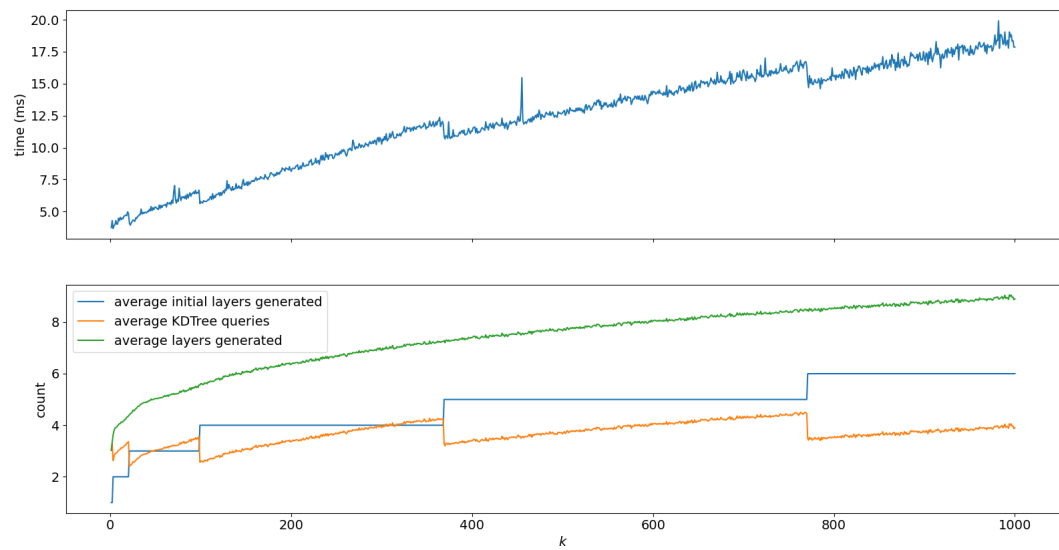


Figure 12 . **Top:** the AMD time in milliseconds averaged over 500 random periodic sets whose three motif points are generated in unit cells with random edge-lengths in $[1, 2]$ and angles in $[\frac{\pi}{3}, \frac{2\pi}{3}]$. **Bottom:** the drops in the AMD running time correspond to the increased number of extra spherical ‘layers’ of generated unit cells, which speed-up further n -d queries [7] for nearest neighbors.

crystal as a point with two coordinates (density, energy). The density is the molecular weight of atoms within a unit cell divided by the unit cell volume. This single-value density is not enough to differentiate crystals, because many non-isometric sets can have the same density. The landscape in Fig. 13 required 12 weeks of supercomputer time [18], because many simulated crystals were not recognized as nearly identical. Even more time and resources are spent on further slower simulation of target properties such as gas adsorption or solubility.

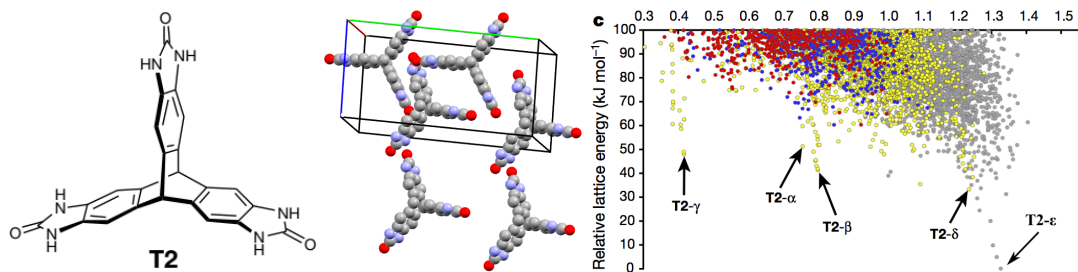


Figure 13 **1st:** T2 molecule. **2nd:** a T2 crystal is obtained from a motif of T2 molecules by periodic translations. **3rd:** energy-vs-density landscape of 5679 simulated T2 crystals [18, Fig. 2d].

The synthesis in a lab started only after an energy landscape in Fig. 13 of 5679 simulated crystals produced by 12-week simulations on a supercomputer hinted at potential stable crystals in downward spikes (imaginable deep minima). To validate this approach, the experimental crystals should be matched with some of 5679 simulated structures. If there was no close match, the expensive simulations missed a real crystal, which is always possible, because the continuous space of all potential crystals in Fig. 13 is randomly sampled.

Until now only the single-value physical density ρ was practically used as a continuous isometry invariant to match crystals. The density ρ can separate nano-porous organic crystals, while inorganic crystals are much denser and can not be well-separated. Using the density ρ

of an experimental crystal, one can search through dozens of simulated crystals in a vertical strip of the energy-vs-density landscape in Fig. 13 over a small interval around ρ to allow for errors. From this strip one takes the simulated crystal with the lowest energy as the best guess. So a result depends on a tolerance error for the density. A final match is confirmed by the non-invariant RMS deviation between finite portions of crystals, see Table 1.

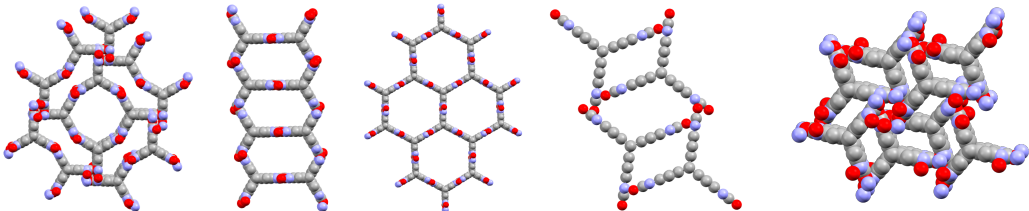


Figure 14 The crystals T2- α , T2- β , T2- γ , T2- δ , T2- ϵ based on the T2 molecule were synthesized for methane capture following the Crystal Structure Prediction output [18] in last picture of Fig. 13.

In the experiments on T2 crystals each of 42 atoms in the T2 molecule was represented by one point. Each of 5679 T2 crystals [18] contains between 1 and 16 T2 molecules in a unit cell, about eight molecules on average and about $m = 370$ motif points per crystal.

The AMD values up to $k = 200$ are computed in 5 min over all 5679 T2 crystals on a modest desktop, while the CSP landscape in Fig. 13 required 12 weeks on a supercomputer. The following closest simulated versions of experimental crystals were manually found in the past, but can now be automatically identified as close neighbors in the clustering dendrogram in Fig. 11: 0186 for T2- α , 0054 for T2- β , 0120 for T2- γ , 0014 for T2- δ , 0001 for T2- ϵ .

Results of [9] and this paper were first presented at the new annual conference MACSMIN (Mathematics and Computer Science for Materials Innovation) in September 2020. The recent result [5] is a continuous and complete invariant (isoset) of all periodic point sets.